Mycobacterium tuberculosis modifies cell wall carbohydrates during biofilm growth with a concomitant reduction in complement activation

Thomas Keating [a,c], Samuel Lethbridge [a], Jon C. Allnutt [a], Charlotte L. Hendon-Dunn [a], Stephen R. Thomas [b], Luke J. Alderwick [c], Stephen C. Taylor [b,1], Joanna Bacon [a,*,1]

[a] *TB Discovery Group, National Infection Service, Public Health England, Porton Down, Salisbury SP4 0JG, United Kingdom*
[b] *Pathogen Immunology Group, National Infection Service, Public Health England, Porton Down, Salisbury SP4 0JG, United Kingdom*
[c] *School of Biosciences, University of Birmingham, Edgbaston, Birmingham B15 2TT, United Kingdom*

ARTICLE INFO

ABSTRACT

The development of new vaccines for TB needs to be underpinned by an understanding of both the molecular and cellular mechanisms of host-pathogen interactions and how the immune response can be modulated to achieve protection from disease. Complement orchestrates many aspects of the innate and adaptive immune responses. However, little is known about the contribution of the complement pathways during TB disease, particularly with respect to mycobacterial phenotype. Extracellular communities (biofilms) of *M. tuberculosis* are found in the acellular rim of granulomas, during disease, and these are likely to be present in post-primary TB episodes, in necrotic lesions. Our study aimed to determine which mycobacterial cell wall components were altered during biofilm growth and how these cell wall alterations modified the complement response. We have shown that *M. tuberculosis* biofilms modified their cell wall carbohydrates and elicited reduced classical and lectin pathway activation. Consistent with this finding was the reduction of C3b/iC3b deposition on biofilm cell wall carbohydrate extracts. Here, we have highlighted the role of cell wall carbohydrate alterations during biofilm growth of *M. tuberculosis* and subsequent modulation of complement activation.

Introduction

Tuberculosis (TB) was responsible for 1.4 million deaths in 2019 and accounts for 25% of all deaths associated with antibiotic-resistance (Global TB Report 2020). There is an urgent need for more effective TB treatments; the disease is challenging to treat, because of limited diagnostic, chemotherapy, and vaccine options. If we are to tackle the disease and achieve the End-TB goals, we need novel, innovative, approaches that enable us to understand host-pathogen interactions and diverse pathologies. It has been recognised that the research needed for the development of new vaccines for TB needs to be underpinned by a better understanding of both the molecular and cellular mechanisms of host-pathogen interaction and how the immune response can be modulated to achieve protection with the use of a new vaccine for TB (Fletcher and Schrager, 2016).

Complement interacts with and orchestrates many aspects of the innate and adaptive immune responses and the activation of complement can elicit a variety of immunological effects, which include the stimulation and modulation of T-cell responses (the focus for TB vaccine development) and subsequent control of inflammatory responses (Watford et al., 2000). Complement is pertinent to TB disease as tubercle bacilli will encounter complement proteins in the lung (Strunk et al., 1988). Complement activation by *M. tuberculosis* can be triggered by the alternative pathway, classical pathway, and lectin pathway (Schlesinger et al., 1990, Bartlomiejczyk et al., 2014, Ferguson et al., 2004). Previous studies have shown that C3b/iC3b deposition onto *M. tuberculosis* is one of the mechanisms utilised by the pathogen to gain access to its intracellular niche (Schlesinger et al., 1990). In the lung, there are limited concentrations of complement components in the alveolar space, but cells can synthesise complement proteins. This may provide a localised complement micro-environment in the lung at the onset of infection (Watford et al., 2000). In human bronchoalveolar lavage fluid (BALF), C3a, C3b, C4a, and C4b are present at comparable concentrations but there is significantly less C1q and Factor B. There is evidence to suggest that the classical pathway is more prominent than the alternative pathway in the lung (Ferguson et al., 2004) but is

reduced in BALF compared to serum (Watford et al., 2000; Ferguson et al., 2004). The alternative pathway is not significantly activated due to low levels of factor D (Watford et al., 2000). Activators of the lectin pathway, ficolin-2, ficolin-3 and mannose-binding lectin (MBL), are detectable but at significantly lower levels in BALF than serum (Vogt et al., 2020).

Complement opsonisation with non-immune sera enhances adherence to monocytes predominantly via complement receptor 3 (CR3) (Schlesinger et al., 1990). Furthermore, entry via complement receptors, of viable complement-opsonised *M. tuberculosis*, does not lead to Ca^{2+} signalling associated with phagosome-lysosome fusion (Malik et al., 2000). Activation of the complement cascade may also provide host protection against *M. tuberculosis* infection. One way is via the release of C5a, which affects the synthesis of key macrophage derived cytokines such as IL-12, IL-1β, TNF-α (Jagannath et al., 2000, Mashruwala et al., 2011). While activation of the late complement pathway and subsequent C5b-9 assembly on the pathogen surface may not result in direct lytic activity as observed with some Gram-negative bacteria, a study utilising C5-deficient mice demonstrated that C5 is required for bacteriostatic control in *ex-vivo* macrophages and is required for granulomatous inflammation (Mashruwala et al., 2011). Studies, which have included the use of C5 and C5a receptor-deficient mice showed that C5 mediated events are essential for generation of a protective granulomatous response against mycobacterial trehalose-dimycolate (TDM) (Borders et al., 2005, Welsh et al., 2012, Welsh et al., 2008). Other cell wall components have also been shown to activate complement. MBL and ficolin-3 directly interact with the surface protein Ag85a (Świerzko et al., 2016) and mannosylated lipoarabinomannan (Bartlomiejczyk et al., 2014) is known to directly activate the lectin pathway. Despite there being evidence that mycobacterial surface components, such as TDM, can activate complement, the relationship between mycobacterial phenotype and complement activation has not been explored in any depth. *M. tuberculosis* is known to modulate the immune response through its complex lipid and sugar rich envelope (Briken et al., 2004, Queiroz and Riley 2017, Gago et al., 2018, Romero et al., 2019). Cell wall modification, due to phenotypic adaptation, such as biofilm growth, is likely to have a role in the alteration of complement activation, particularly as an accumulation of free mycolate is associated with *M. tuberculosis* pellicle biofilms (Ojha et al., 2008). TB is a complex, chronic disease, resulting from a plethora of interactions between heterogeneous tubercle bacilli and a variety of host cells in the lung and other compartments of the body. During chronic infection, *M. tuberculosis* persists in biofilms located in extracellular multicellular micro-colonies located in the acellular rim of human and guinea pig granulomas (Grosset 2003, Hunter 2011, Hunter 2016). Our study aims to understand more about the interactions between *M. tuberculosis* biofilms and complement activation and to determine which mycobacterial cell wall components that are altered during biofilm growth, contribute to modulation of the complement response. We used human complement deposition assays to determine which pathways were altered in their activation, in biofilms compared to planktonically-grown *M. tuberculosis* (Brookes et al., 2018). There is no significant alternative pathway activity in the lung due to low levels of factor B (Watford et al., 2000). To reflect this, samples were incubated with 10% complement, where all pathways are active and with 2% complement where the alternative pathway is inhibited. Lipids and carbohydrates were differentially extracted, from the two bacterial phenotypes, and biochemical analyses were performed to determine their composition. Specific interactions between extracted cell wall components and different complement activators were explored using quantitative enzyme linked immunosorbent assays (ELISA).

Materials and methods

M. tuberculosis planktonic and biofilm culture

All cultures were grown in modified Sauton medium with the following ingredients: KH_2PO_4 0.05 mg mL^{-1}, $MgSO_4$ 7H$_2$O 0.5 mg mL^{-1}, citric acid 2.0 mg mL^{-1}, ferric ammonium citrate 0.05 mg mL^{-1}, glycerol 75.6 mg mL^{-1}, asparagine 4.0 mg mL^{-1} and adjusted to pH 7.4). The inoculum used for all cultures (planktonic or biofilms) were samples taken from steady state fast-growth chemostat cultures grown in CMM MOD2 medium (James et al., 2000, Bacon et al., 2004). Planktonic cultures were grown in aerated flasks shaking at 200 rpm at 37 °C for 7 days, from a starting optical density of 0.05 OD$_{540nm}$. Biofilms were grown in 24-well plates. These were inoculated using starter cultures, containing modified Sauton medium that had been inoculated with chemostat culture to an optical density of 0.05 OD$_{540nm}$ and grown for 7 days, whilst shaking at 200 rpm at 37 °C. Each well was inoculated with 2 mL of culture. These were incubated for 5 weeks, statically, at 37 °C in an airtight container. Planktonic cultures were harvested by pelleting at 3060g for 10 min and biofilm cultures were harvested by scraping biomass from the air–liquid interface using sterile disposable spatulas, into a glass tube. Cell biomass was dried down, using a Genevac EZ-2 plus evaporator, in preparation for extractions. An equivalent quantity of biomass from each culture type was used for further extractions and complement deposition assays. Biomass scraped from the wells of eight plates, were pooled to give a single replicate biofilm sample. Biomass was quantified by optical density or dry weight, depending on the analyses.

Scanning electron microscopy of intact M. tuberculosis biofilms

M. tuberculosis biofilms were cultured in 24-well plates containing sterile plastic coverslips, cut to size, and placed into each well. After 5 weeks of biofilm growth the coverslips were removed and fixed in 4% formaldehyde (v/v in water) followed by ethanol/solvent dehydration: formaldehyde was carefully removed and replaced with 2% osmium tetroxide for 2 h at room temperature for secondary fixation. Biofilms were then dehydrated through graded ethanol solutions for 15 min at room temperature sequentially at 25%, 50%, 75%, or 100% concentration. Following this, the coverslips were dehydrated with 100% Hexamethyldisilane for 15 min at room temperature; this step was repeated. Coverslips were then air-dried and mounted on SEM stubs using double-sided adhesive carbon discs. The mounted coverslips/pellicles were coated with gold to a thickness of 10 nm,using an ion beam sputter coater (AtomTech 700 series Ultra Fine Grain Coating Unit). The scanning electron microscope used was a Philips / FEI XL30 FEG SEM operated at 4 kV accelerating voltage and a working distance of 10.2 mm.

Non-covalent carbohydrate and mAGP extraction

The method described by Besra et al., (Besra et al., 1998) was followed. Biomass was harvested from three replicate planktonic or biofilm *M. tuberculosis* samples, inactivated by autoclaving at 126 °C for 30 min, and evaporated to dryness using a Genevac EZ-2 plus evaporator. Planktonic or biofilm biomass was quantified by dry weight to ensure equivalent quantities of planktonic and biofilm biomass were used in the extractions. A quantity of 2 g of biomass was used in each extraction, consisting of pooled cell pastes from replicate cultures. Samples were heated under reflux with 10 mL ethanol–water (1:1) at 75 °C for 4 h. Samples were then left to cool to room temperature, spun at 3000 g for 15 min, and the supernatant was removed into fresh tubes. The pellet was topped up to 10 mL with ethanol–water (1:1) and the heating step and centrifugation were repeated. The supernatants were vacuum-dried, and the pellets were recombined in phenol saturated with PBS. The samples were heated at 75 °C for 30 min and left to cool to room

temperature. The phenol and aqueous layers were separated by centrifugation at 3000 g. The aqueous layer was removed into a semi-permeable dialysis membrane (MWCO 3500). The samples were dialysed overnight with running tap water and left in distilled water for 1 h to remove salts from the tap water. Samples were transferred into clean pre-weighed glass tubes and were subsequently dried. The remaining pellet from the ethanol reflux was used for mAGP extraction. 2% SDS (w/v in PBS) was added to planktonic and biofilm pellets that were remaining from the ethanol reflux step of the carbohydrate and lipoglycan extraction. Samples were heated under reflux at 95 °C overnight. Following this, the samples were washed with water, pelleted, washed with 80% acetone (v/v in water), pelleted, washed with 100% acetone, and dried.

Carbohydrate analyses

The method described in Bacon et al. (2014) and Birch et al. (2010) was followed. Planktonic and biofilm carbohydrate and mAGP extracts were treated with 2 M Trifluoroacetic acid (TFA). 200 μL of 2 M TFA was added to 0.5 mg mAGP or carbohydrate extracts. Samples were heated to 120 °C for 1.5 h under reflux and allowed to cool to room temperature. The acid was evaporated using a sample concentrator. 100 μL of 10 mg mL^{-1} Sodium borate (NaBH$_4$) in 1:1 ethanol: NH$_4$OH (1 M) was added to each sample and left capped at room temperature overnight. 3 drops of glacial acetic acid were added to each sample and evaporated. Three drops of 10% glacial acetic acid in methanol were added then evaporated. This step was repeated. Three drops of 100% methanol were added and evaporated. This step was repeated. 100 μL acetic anhydride was added and this was heated at 120 °C for 1 h. After allowing the sample to cool to room temperature, 100 μL of toluene was added to the samples, and this was evaporated. 2 mL of chloroform and 2 mL of water were added to each sample. The lower organic layer was transferred into a fresh tube using a glass pipette and dried for gas chromatography analysis. Gas chromatography analysis was performed using a Thermoquest Trace GC 2000. Samples were injected in the splitless mode. The column used was a DB225 (Supelco). The oven was programmed to hold at an isothermal temperature of 275C for a run time of 15 min. All the data were collected and analysed using Xcaliber (v.1.2) software.

Quantitative ELISA

A previously published ELISA method was used with modifications (Bahia El Idrissi et al., 2015). Three biological replicates of planktonic or biofilm *M. tuberculosis* carbohydrate extracts at 15 mg mL^{-1} were diluted in 1 mL of carbonate buffer (Sigma carbonate/bicarbonate capsule in 100 mL distilled water) to a final concentration of 25 μg mL^{-1}. 100 μL of buffer was added to eight wells of a microtitre plate to ensure 2.5 μg of carbohydrate per well. Seven-point standard curves were generated using 1:4 serial dilutions of human purified C3 (CompTech). Microtitre plates were sealed and left at 4 °C overnight to bind carbohydrates and protein standards to the bottom of the wells. The buffer was removed by inverting the plate. The plate was blocked by adding 100 μL of 10% BSA (v/v in PBS) to each well and incubating for 1 h. The wash step was repeated and 100 μL of PBS containing 0.05% Tween 20 was added to each well and washed again. 100 μL of complement binding buffer (CBB; 1.76 mM MgCl2, 0.25 mM CaCl2, 145.4 mM NaCl), 2% complement in CBB or 10% complement in CBB were added to respective wells and incubated for 1 h at 37 °C. Plates were washed as previously described. For C3b/iC3b ELISAs, 100 μL of (1:500) pAb anti-C3c HRP (Abcam) in CBB was added to each well. The plate was sealed and incubated for 1 h at room temperature. Plates were quantified using a Multiskan EX plate reader at 450 nm with Ascent software. Five-parameter standard curves to quantify bound C3b/iC3b with absorbance values were generated using GraphPad Prism software (version 9.0). Significant differences in C3b/iC3b deposition on planktonic or biofilm carbohydrate extracts was determined using Welch's *t*-test in GraphPad Prism software.

Dispersion of M. tuberculosis cultures

To provide biomass samples for complement deposition and analyses by flow cytometry, biomass was dispersed by agitation with 4 mm glass beads (Villeneuve et al., 2003, N'Diaye et al., 1998) with the following modifications. Live *M. tuberculosis* planktonic pellets or scraped biofilms were agitated with sterile 4 mm glass beads, which had been added at a ratio of approximately 5:1 bead volume: pellet volume. The samples were mixed using a vortex for 1 min, suspended in PBS and left to sediment for 10 min. The liquid was poured into fresh tubes and the suspension was spun at 200 g. The supernatants containing the dispersed cells were aliquoted into cryovials and frozen at −80 °C until required.

C3b/iC3b deposition ± mAb C1q assay

Viable, thawed planktonic and biofilm *M. tuberculosis* from glass-bead treated stocks, were diluted to stocks of 0.2 OD$_{540nm}$ in complement binding buffer (CBB). This buffer was made by dissolving a complement fixation diluent tablet (Oxoid, UK) in PBS containing 2% bovine serum albumen. CBB contained 1.76 mM MgCl2, 0.25 mM CaCl2, 145.4 mM NaCl. IgG-depleted exogenous pooled human complement was pre-incubated for 20 min at 4 °C with PBS (control) or mouse anti-human C1q mAb (Hycult Biotech, Netherlands) that had been diluted 5-fold. Zymosan was used as an assay control (yeast cell wall extract; Complement technologies) and was also diluted to a stock at 0.2 OD$_{540nm}$ in complement binding buffer (CBB). A volume of 45 μL of either bacteria or zymosan was added to wells in the plate. To 2% complement wells, 2.5 μL of IgG-depleted exogenous pooled human complement-PBS/mAb anti C1q (4:1) was added along with 52.5 μL of CBB. To 10% complement wells, 12.5 μL of IgG-depleted exogenous pooled human complement-PBS/mAb anti C1q (4:1) was added along with 42.5 μL CBB. The plate was incubated at 37 °C for 45 min at 900 rpm. The plate was centrifuged at 3060g for 5 min and each well was washed with 200 μL CBB. The plate was spun again at 3060 g and re-suspended in 4% PBS-formaldehyde, to inactive the bacteria. The plate was spun, by centrifugation, at 3060 g and re-suspended in CBB. This spin was repeated and re-suspended in 200 μL of CBB containing FITC rabbit anti-human C3c pAb (Abcam, UK) at a 500-fold dilution. The plate was incubated at 4 °C for 20 min, spun at 3060 g for 5 min, and washed twice with PBS, before being analysed by flow cytometry using a CyAN ADP Analyser flow cytometer (Beckman-Coulter, USA). Compensation was performed using Summit 4.3 software (Beckman-Coulter, USA) from single conjugate sample FCS files and the magnitude of C3b/iC3b deposition was measured by calculating integrated median fluorescence intensity (median fluorescence × % positive cells) for each sample. The iMFI of bacteria + conjugate only negative control wells were subtracted from each sample to remove the contribution of background fluorescence to net iMFI values. For statistical analysis, ≥3 biological replicate planktonic and biofilm samples were compared by performing t-tests corrected for multiple comparisons by false discovery rate (Benjamini et al., 2006) with Q = 5% using GraphPad Prism software.

MBL, C1q and Ficolin-3 binding assays

Viable, thawed, planktonic or biofilm *M. tuberculosis* from glass-bead treated stocks, were diluted to 0.2 OD$_{540nm}$ in CBB. 55 μL of CBB was added to control wells and 54 μL added to MBL/C1q/ficolin-3 wells. 45 μL of bacteria was added to designated wells. Recombinant MBL (R&D systems) (100 μg mL^{-1}), recombinant ficolin-3 (R&D systems), or human purified C1q (Comp Tech) were added to designated wells to give a final concentration of 1 μg mL^{-1} in 100 μL. Plates were incubated at 900 rpm at 37 °C for 45 min, spun at 3060g for 5 min, and washed with 200 μL CBB per well. Plates were spun at 3060g for 5 min and re-suspended in either 1:100 mouse anti-human MBL (Hycult), 1:500

mouse anti-human C1q (Quidel), or 1:100 mouse anti-human Ficolin-3 (Hycult) in CBB or CBB only, and incubated for 20 min at room temperature. Plates were spun at 3060g for 5 min and washed with 200 µL CBB per well. Plates were spun at 3060 g for 5 min and re-suspended in 1:500 Goat Anti-Mouse IgG (H + L) Fluorescein (FITC)-AffiniPure F(ab') 2 Fragment antibody in CBB or CBB only and incubated for 20 min at room temperature. Plates were spun at 3060 g for 5 min and washed with 200 µL filter-sterilised PBS per well and this step was repeated. Plates were spun at 3060g for 5 min and re-suspended in 200 µL 4% formaldehyde in PBS per well and sealed with 70% ethanol-soaked plate sealers. Plates were sprayed with 70% ethanol and incubated at room temperature for 1 h to inactivate the bacteria in the wells. For statistical analyses of the MBL, C1q, and ficolin-3 experiments, ≥3 biological replicate *M. tuberculosis* planktonic and biofilm samples were compared by performing two-tailed Welch's t-tests using GraphPad Prism software.

Results

There is reduced complement activation by biofilm bacteria compared to planktonic bacteria

The impact of biofilm growth on complement activation was determined in pellicle-grown *M. tuberculosis* by comparing three independent replicate biofilm and planktonic growths. IgG-depleted pooled human plasma was used as a complement source and two-colour flow cytometry analyses used to quantify complement-deposition onto the bacterial surface (Brookes et al., 2018). The complement source was used at 10% or 2% (final concentration in the assay) in order to assess activation in either the presence of all three pathways (10% complement) or the presence of only the classical and lectin pathways (2% complement). Reduced activation at 2% complement is due to the absence of the alternative pathway because of a lack of available Factor D (Volanakis et al., 1985). A reduction in the magnitude of C3b/iC3b deposition (Fig. 1A) was observed on biofilm bacteria compared to planktonic bacteria in both the presence (10% complement P = 0.023) and absence (2% complement P = 0.008) of the alternative pathway. Biofilms also resulted in significantly reduced deposition of C5b-9 (Fig. 1B) at both complement concentrations (10% complement P = 0.003, 2% complement P = 0.0003). However, the difference was greater in the absence of the alternative pathway, which is a physiological condition relevant to the lung.

Complement deposition on biofilm M. tuberculosis is more dependent on the classical pathway and show reduced lectin pathway activation

The contribution of individual activation pathways to the deposition

of C3b/iC3b on the surface of *M. tuberculosis* was assessed. By blocking C1q using a specific monoclonal antibody and therefore preventing classical pathway activation, deposition of C3b/iC3b (Fig. 2) was partially inhibited (P < 0.05). This reduction appeared to be greater in the absence of the alternative pathway (P < 0.02). Despite this reduction, significant C3b/iC3b deposition was observed in the absence the classical pathway (minus C1q) and the alternative pathway on both planktonic and biofilm bacilli thereby showing the significance of the lectin pathway for C3b/iC3b deposition on tubercule bacilli. In the absence of the alternative pathway, approximately a third of the C3b/iC3b deposited on planktonic cells was classical pathway-mediated, while the classical pathway contributed two-thirds on biofilm cells; as evidenced by the loss of C3b/iC3b deposition in the absence of C1q. Taken together, these results show that all three pathways contribute to complement activation on planktonic and biofilm bacteria. However, they also suggest that the lectin pathway has a reduced role compared to the classical pathway in initiating complement activation onto biofilm cells and is the major pathway for activation on planktonic cells.
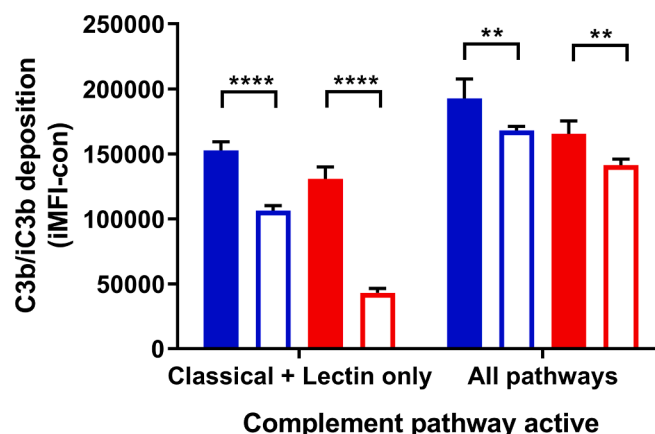

Fig. 2. Complement activation by planktonic and biofilm *M. tuberculosis*. Mean net C3b/iC3b deposition on either biofilms (red bars) or planktonic bacteria (blue bars) with (unfilled bars) or without (shaded bars) pre-incubation with C1q monoclonal antibody (inhibition of the classical pathway) at either 2% complement (Classical and Lectin only) or 10% complement (All pathways). Error bars show standard deviation (n = 4). Zymosan was used as an assay control in the deposition assays, with an integrated median fluorescence intensity (iMFI ± SD) = 269371 ± 10172 (classical + lectin only) and iMFI ± SD 423839 ± 25796 (all pathways). (For interpretation of the references to colour in this figure legend, the reader is referred to the web version of this article.)
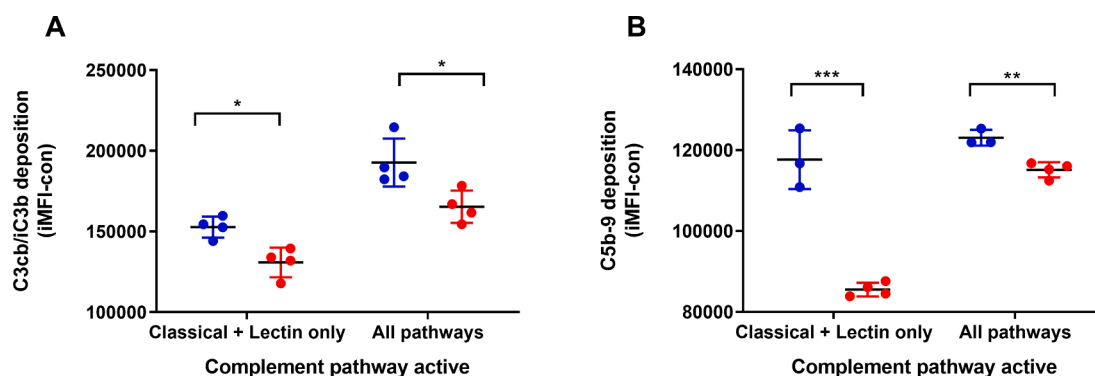

Fig. 1. Complement activation by planktonic and biofilm *M. tuberculosis* Mean net deposition (mean fluorescence intensity of the test minus the conjugate-only control) on planktonic and biofilm *M. tuberculosis* for C3b/iC3b (A) and C5b-9 (B). Error bars show standard deviation (n = 4). Zymosan was used as an assay control in the deposition assays, with an integrated median fluorescence intensity (iMFI ± SD) = 269371 ± 10172 (classical + lectin only) and iMFI ± SD 423839 ± 25796 (All pathways).

There is reduced binding of MBL and C1q to M. tuberculosis biofilms

We subsequently quantified the direct binding of classical and lectin pathway activators (C1q and MBL respectively), to planktonic and biofilm *M. tuberculosis* bacteria. In addition, we investigated the binding of ficolin-3, which is a key ficolin and activator of the lectin pathway and is present in the human lung (Watford et al., 2000). MBL deposition was reduced on biofilm *M. tuberculosis* by 58.9% compared to planktonic bacteria (P = 0.018, Fig. 3A). Similarly, direct binding of C1q was also reduced in the biofilm phenotype (P = 0.046 Fig. 3B). Ficolin-3 deposition was also reduced on biofilms, but this was not a statistically significant (P = 0.084) (Fig. 3C).

Biofilm-grown M. tuberculosis has an altered carbohydrate composition in the cell wall

We observed the accumulation of extracellular matrix (ECM) in biofilms by scanning electron microscopy (Fig. 4). Analyses of the total lipids confirmed previous findings that there was an accumulation of free mycolic acids. Cell wall associated carbohydrates were also extracted. The relative proportions of the constituent sugars in the carbohydrate extracts and mycolyl-arabinogalactan-peptidoglycan complex (mAGP) were determined by chemically modifying them to produce alditol acetate derivatives, which were subsequently analysed by gas chromatography, as described previously (Birch et al., 2010, Bacon et al., 2014). The relative proportions of arabinose, mannose, and glucose, from two independent total sugar analyses of planktonic carbohydrate extracts were 17.83 ± 8.65 %, 33.75 ± 0.39 %, and 48.43 ± 8.26 %, respectively. We observed a different pattern in the relative
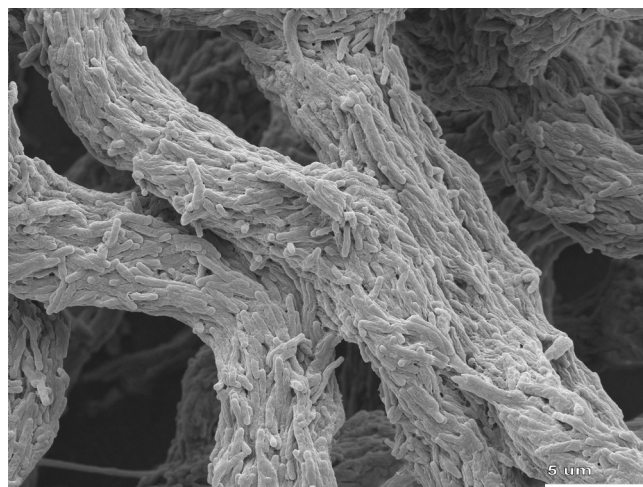

Fig. 4. Scanning electron microscopy of *M. tuberculosis* pellicle biofilms at 5 weeks of growth. Samples were prepared by fixation with formaldehyde followed by secondary fixation with 2% osmium tetroxide and graduated solvent dehydration. Magnification x4000.

proportions of the sugars for biofilm carbohydrate extracts; arabinose (34.89 ± 0.65 %), mannose (50.33 ± 6.99 %), and glucose (14.78 ± 6.34 %). To gain a clearer understanding of these constituent sugar changes, sugar: sugar ratios were determined (Fig. 5A). The proportion of glucose relative to arabinose and mannose was lower in the biofilms compared to planktonic-grown cells, while the proportion of arabinose relative to
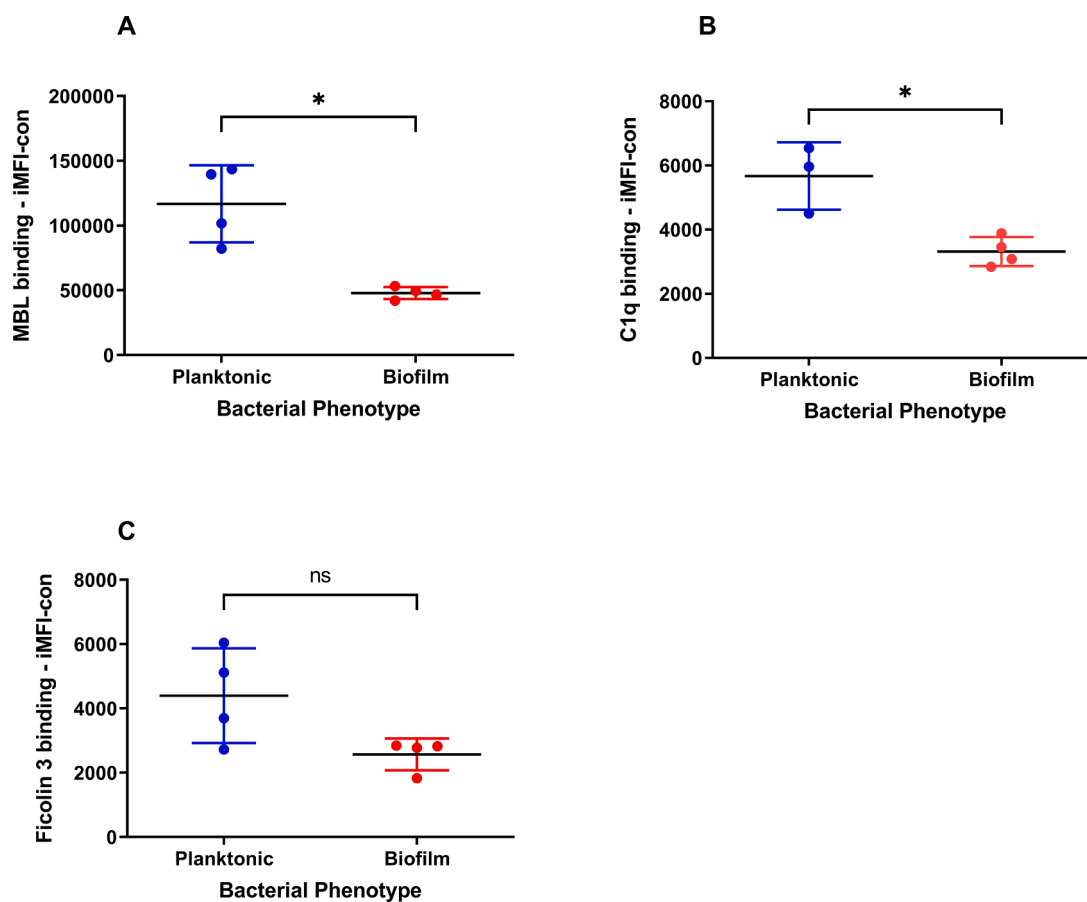
Fig. 3. Binding of complement activators to planktonic and biofilm *M. tuberculosis*. Mean net binding to planktonic or biofilm *M. tuberculosis* of mannose lectin binding protein (MBL) (A) C1q (B) or ficolin-3 (C). Error bars show standard deviation (n = 4). Zymosan was used as an assay control in the deposition assays, with an integrated median fluorescence intensity (iMFI ± SD) = 82216 ± 12485 (MBL-binding).
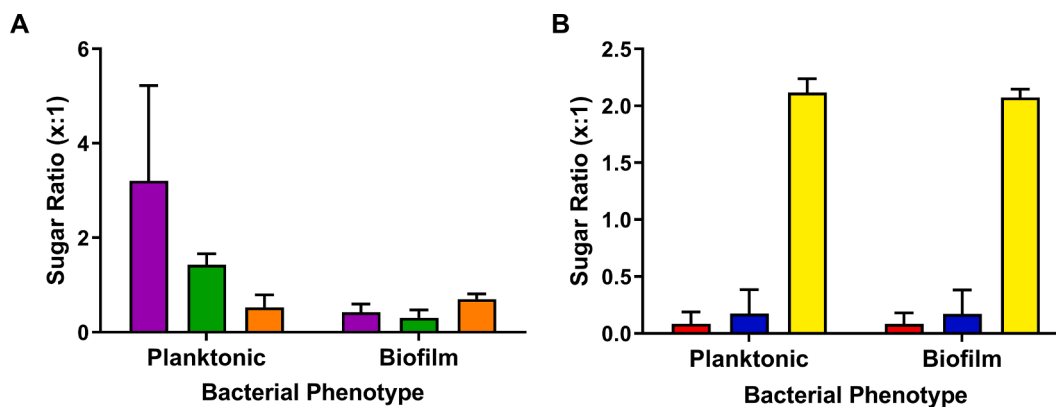
Fig. 5. Sugar analysis of *M. tuberculosis* planktonic and biofilm carbohydrates and mycolyl-arabinogalactan-peptidoglycan (mAGP) cell wall extracts. (A) Mean constituent sugar: sugar ratios of planktonic and biofilm *M. tuberculosis* carbohydrate extracts; glucose: arabinose (x:1; purple), glucose: mannose (x:1; green), arabinose: mannose (x:1; orange). (B) Mean constituent sugar: sugar ratios of planktonic and biofilm mAGP extracts; rhamnose: arabinose (x:1; red) rhamnose: galactose (x:1; blue), arabinose: galactose (x:1; yellow). Error bars show standard deviation (n = 2). (For interpretation of the references to colour in this figure legend, the reader is referred to the web version of this article.)

mannose remained unchanged (Fig. 5A). Ratios for rhamnose: arabinose, rhamnose: galactose, and arabinose: galactose in the mAGP complex were equivalent for the two phenotypes (Fig. 5B). These sugar ratios served as internal controls by confirming that equal quantities of biomass from the two cell states, were used in these comparisons. Taken together, these results show a reduction in glucose in the *M. tuberculosis* biofilm carbohydrate extracts compared to extracts from planktonically grown bacteria. As α-glucan is the only cell wall sugar (captured by these carbohydrate extractions/analyses) to contain glucose, it follows that the prevalence of α-glucan is likely to be diminished during the formation of mycobacterial biofilms under the pellicle growth conditions, described in this study.

Deposition of C3b/iC3b was significantly reduced on carbohydrates extracted from biofilm compared to planktonic M. Tuberculosis

To determine how the altered carbohydrates in biofilm extracts modulate complement and which pathways were differentially activated, we measured the level of C3b/iC3b deposition on carbohydrate extracts from biofilms compared to extracts from planktonic growth using a quantitative enzyme-linked immunosorbent assay (ELISA). There was less C3b/iC3b deposition on biofilm carbohydrates compared to planktonic carbohydrates, though this difference was only observed in the absence of the alternative pathway (P = 0.043, Fig. 6A) and not when all three pathways were active (P = 0.433, Fig. 6B), suggesting

that additional amplification provided by the alternative pathway may have saturated the discernible differences in activation between the biofilm and planktonic carbohydrates. The reduced C3b/iC3b deposition elicited by biofilm carbohydrates is commensurate with both the observed reduction of C3b/iC3b deposition on biofilm bacilli and a reduction in the contribution of the lectin pathway in initiating complement activation on whole bacteria from biofilms, compared to planktonically grown bacteria. This highlights the role of carbohydrate alterations during biofilm growth of *M. tuberculosis* and subsequent modulation of the innate immune response.

Discussion

There is reduced complement deposition on biofilm M. tuberculosis

Previous studies have suggested C3b/iC3b deposition on *M. tuberculosis* is one of the mechanisms utilised by the pathogen to gain access to its intracellular niche (Schlesinger et al., 1990) and that entry via complement receptors enables the pathogen to avoid phagosome-lysosome fusion (Malik et al., 2000). In addition to the intracellular phase, there is much evidence now that *M. tuberculosis* persists in an extracellular state in the periphery of cavitary lesions. These extracellular communities are found in the acellular rim of granulomas, have been observed in cavities in lung resections from TB patients, and are likely to be present in post-primary TB episodes in necrotic lesions
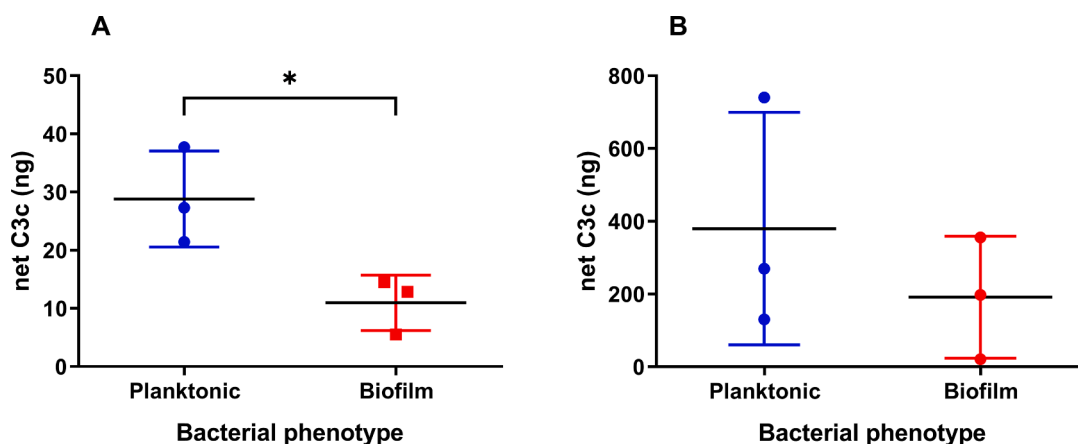
Fig. 6. Quantitative ELISA measuring complement deposition on *M. tuberculosis* carbohydrate extracts. C3b/iC3b deposition on planktonic and biofilm carbohydrate extracts incubated with 2% complement (A; alternative pathway inactive) or 10% complement (B; all pathways active). Error bars show standard deviation (n = 3).

(Grosset J. 2003, Hunter RL. 2011, Hunter RL. 2016). Nyka *et al.* demonstrated that these extracellular bacilli resemble biofilms formed by other pathogenic bacteria that cause extracellular infection (Nyka 1967, Nyka and O'Neill 1970 Nyka 1974). These extracellular *M. tuberculosis* communities resemble bacterial biofilms. Extracellular, drug-tolerant, bacilli, have also been observed in drug-treated animals, such as guinea pigs that develop necrotic granulomas (Lenaerts et al., 2007, Lenaerts et al., 2015, Lanoix et al., 2015). Further confirmation is needed as to whether drug-treatment induces the presence of these biofilm-like communities. The extracellular matrix (ECM) around these acellular rims, typical of biofilms, has been shown to contain *M. tuberculosis* mycolic acids, likely secreted by bacilli (Hoff et al., 2011). *M. tuberculosis* can alter these outer-surface molecules and orchestrate a variety of modulated host-responses that dictate the outcome of disease, and the effectiveness of treatment. We need to understand more about this mycobacterial phenotype, other cell wall components that are modified in a biofilm, and their host-pathogen-interaction, so that we can target biofilms with new treatment strategies. With a focus on complement, in this study, the reduction in complement deposition and binding of MBL and C1q on pellicle biofilms, suggest that the organism could be resisting phagocytosis through reduction in the binding of opsonin C3b. Further to this, a reduction in C3b generation and binding would also lead to a reduction in the release of the potent immuno-modulatory anaphylatoxins C3a and C5a, in turn, regulating excessive inflammation and activation of cellular responses, which warrant further investigation, as possible targets for the control of necrotic inflammation.

Complement activation on biofilm M. tuberculosis is more dependent on the classical pathway and shows reduced lectin pathway activation

Irrespective of phenotype, we have observed that activation of the complement system by *M. tuberculosis* can occur via antibody-independent activation of classical pathway. The current paradigm is that antibodies are required for classical pathway activation. However, we have shown that for *M. tuberculosis* the classical pathway can be initiated by direct binding of C1q to the cell surface. C1q was blocked using a specific anti-C1q monoclonal antibody and there was a significant reduction in C3b/iC3b deposition on both biofilm and planktonic bacteria, this was especially pronounced on biofilm bacteria. Raised C1q levels have been measured in patients with TB (Cai et al., 2014) as compared to other respiratory diseases such as pneumonia and sarcoidosis. Direct binding of C3 either via the classical pathway or the alternative pathway (depending on the sera concentration) has been observed using sera or bronchial lavage from non-immune patients (Ferguson et al., 2004). Taken together, these data are indicative of a role for the classical pathway in TB disease.

We also observed activation of the lectin pathway by selective inhibition of the alternative and classical pathways and by direct binding of MBL and ficolin-3 to the planktonic or biofilm bacilli. This is supported by previous evidence that activation of the lectin pathway can occur through interaction of cell surface protein Ag85a and lipoarabinomannan with MBL and ficolins (Bartlomiejczyk et al., 2014, Świerzko et al., 2016). With such a carbohydrate-rich cell surface it is unsurprising that *M. tuberculosis* activates the lectin pathway. What has not been shown previously is the impact of growth phenotype on the modulation of lectin pathway activation. There is a significant reduction in MBL-binding on biofilm bacteria compared to planktonic bacilli with a concomitant reduction in lectin pathway activation. Biofilm formation has been associated with reduced activation of the complement system in another respiratory mycobacterial species such as *Mycobacterium abscessus* and there are examples of other bacterial biofilms, which demonstrate modulated complement activation, particularly reduced C3b deposition, via a variety of pathogen-specific mechanisms (Rhoades et al., 2009). Deposition of C3b and C1q-binding to the bacterial surface of *Streptococcus pneumoniae* biofilms is impaired, enabling

pneumococcal biofilms to avoid the activation of the classical pathway (Domenech et al., 2013). *Pseudomonas aeruginosa* growing planktonically resulted in a stronger activation of complement than biofilms (Jensen et al., 1993), which could be inactivating the complement system by secreting alkaline protease and elastase (Kharazmi et al., 1991). Biofilms are likely to have a plethora of wide-reaching interactions and effects on the innate immune response. *Staphylococcus pneumoniae* biofilms also impair phagocytosis and this may be due to the reduction of C3b deposition. We know that complement deposition enables phagocytosis of *M. tuberculosis*. However, we do not yet know the impact of a biofilm phenotype on the interplay between complement, cell-mediated immunity, and the adaptive humoral response.

In our study, and in patient studies, it is challenging to determine the contribution of each pathway, as both the classical and lectin pathways are innately activating complement. Following a similar approach to the inhibition of the classical pathway by blocking C1q, we would need to inhibit the lectin pathway in order to understand the specific contribution that each pathway is making. This could potentially be achieved by saturating (thereby by blocking) the activation of MBL complement with mannose. However, this would not completely inactivate the lectin pathway as we have also shown binding of ficolin 3, which will not bind to mannose and therefore remain active (Gout et al., 2010).

M. tuberculosis biofilms show altered complement activation through the modification of carbohydrates

To investigate the physiological differences between biofilm and planktonic bacilli that result in altered complement-pathogen interactions, we explored the differences in the composition of cell surface components. We observed changes in the lipids composition and saw an accumulation of free mycolate; the association of free mycolate with the extracellular material of mycobacterial pellicles is now widely accepted (Ojha et al., 2008). Polysaccharides are often associated with the extracellular matrix in other bacteria (Limoli et al., 2015). However, there have been very few studies that describe carbohydrate changes in the *M. tuberculosis* biofilm. Given the role of bacterial sugars in the activation of the lectin pathway and the differences in the contribution of this pathway to complement activation between the two phenotypes, we chose to focus on the analysis of carbohydrate changes in the cell wall. The outermost non-covalently bound cell wall carbohydrate/lipoglycan fractions were analysed (so could also contain ECM carbohydrates) and highlighted a reduction of a glucose-containing carbohydrate in the biofilms; this is likely to be α-glucan given the type of extraction process that was used here. Previous linkage analysis of *M. tuberculosis* H37Rv cultured in Sauton medium as pellicle biofilms only identified α-glucan (Ortalo-Magné et al., 1995) further supporting the fact that glucose identified, here, is derived solely from α-glucan. Further work is in progress to determine the precise biochemical composition of these carbohydrates. No changes were observed in the proportion of arabinose: mannose confirming that there were no alterations in the lipoglycan composition or arabinomannan between the two phenotypes, such as elongation of the arabinan chain, as observed under a nutrient starved non-replicating state (Bacon et al., 2014). Previously, a loosely bound capsule has been associated with *M. tuberculosis*, comprising carbohydrates, particularly α-glucan (Lemassu and Daffe 1994) which is expressed both *in vitro* and *in vivo* (Schwebach et al., 2002). These capsular polysaccharides, including α-glucan, will mediate the non-opsonic binding of *M. tuberculosis* H37Rv to CR3 (Cywes et al., 1997), which may be favourable to the intracellular survival of the tubercle bacillus. However, the role of capsule in pathogenesis has not been determined. Here, the reduced C3b/iC3b deposition elicited by biofilm carbohydrates was consistent with both the observed reduction of C3b/iC3b deposition on biofilm bacilli and a reduction in the contribution of the lectin pathway in initiating complement activation on whole bacteria from biofilms, compared to planktonically grown bacteria. This highlights the role of carbohydrate alterations during

biofilm growth of *M. tuberculosis* and the subsequent modulation of the innate immune response. Although it is challenging to directly compare the levels of C3b/iC3b deposition between the experiments with whole bacteria (Fig. 1) and carbohydrates, it appears that the differences in activation between biofilms and planktonic bacteria were greater on whole bacteria. This could be explained by the contribution of other bacterial components (such as cell wall proteins and lipids), to the response present in whole bacteria, and not in the carbohydrate fractions. Given that C3b/iC3b deposition onto *M. tuberculosis* is one of the mechanisms utilised by the pathogen to gain access to its intracellular niche (Schlesinger et al.,1990) and that entry via complement receptors enables the pathogen to avoid phagosome-lysosome fusion, reduction of α-glucan may be a mechanism by which *M. tuberculosis* avoids uptake during an extracellular phase of its life cycle. If we also consider these extracellular bacterial biofilms in the context of TB transmission; expectorated *M. tuberculosis* biofilm bacteria could be entering the lung environment of a new host where the alternative pathway is not active. Complement activation leads to the release of the anaphylatoxin C5a, which is required for tuberculosis control (Jagannath et al., 2000, Mashruwala et al., 2011). Reduction of complement activation by these bacteria may provide an advantage in the establishment of infection.

Concluding remarks

Our study reveals that *M. tuberculosis* cultured as a pellicle biofilm leads to reduced complement activation. We show here that *M. tuberculosis* biofilms modify their cell wall carbohydrates. Consistent with this finding is reduced classical and lectin pathway activation, which is associated with reduction of C3b/iC3b deposition on biofilm carbohydrate extracts. We have highlighted the role of carbohydrate alterations during biofilm growth of *M. tuberculosis* and subsequent modulation of the innate immune response, which may be one mechanism by which, *M. tuberculosis* avoids phagocytosis in establishing an extracellular state in the lung.

CRediT authorship contribution statement

Thomas Keating: Methodology, Formal analysis, Investigation, Writing – review & editing. **Samuel Lethbridge:** Methodology, Writing – review & editing. **Jon C. Allnutt:** . **Charlotte L. Hendon-Dunn:** . **Stephen R. Thomas:** Methodology, Writing – review & editing. **Luke J. Alderwick:** Methodology, Resources, Writing – review & editing, Supervision. **Stephen C. Taylor:** Conceptualization, Methodology, Formal analysis, Resources, Writing – review & editing, Supervision, Funding acquisition. **Joanna Bacon:** Conceptualization, Methodology, Resources, Writing – original draft, Writing – review & editing, Supervision, Funding acquisition.

Declaration of Competing Interest

The authors declare that they have no known competing financial interests or personal relationships that could have appeared to influence the work reported in this paper.

References

Global tuberculosis report 2020. https://www.who.int/teams/global-tuberculosis-programme/tb-reports/global-tuberculosis-report-2020.

Bacon, J., James, B.W., Wernisch, L., Williams, A., Morley, K.A., Hatch, G.J., Mangan, J. A., Hinds, J., Stoker, N.G., Butcher, P.D., Marsh, P.D., 2004. The influence of reduced oxygen availability on pathogenicity and gene expression in *Mycobacterium tuberculosis*. Tuberculosis (Edinburgh, Scotland) 84, 205–217. https://doi.org/10.1016/j.tube.2003.12.011.

Bacon, J., Alderwick, L.J., Allnutt, J.A., Gabasova, E., Watson, R., Hatch, K.A., Clark, S. O., Jeeves, R.E., Marriott, A., Rayner, E., Tolley, H., Pearson, G., Hall, G., Besra, G.S., Wernisch, L., Williams, A., Marsh, P.D., 2014. Non-replicating *Mycobacterium tuberculosis* elicits a reduced infectivity profile with corresponding modifications to the cell wall and extracellular matrix. PLoS ONE 6;9(2):e87329. https://doi.org/10.1371/journal.pone.0087329.

Bahia El Idrissi, N., Das, P.K., Fluiter, K., Rosa, P.S., Vreijling, J., Troost, D., Morgan, B.P., Baas, F., Ramaglia, V., 2015. *M. leprae* components induce nerve damage by complement activation: identification of lipoarabinomannan as the dominant complement activator. Acta Neuropathol. 129, 653–667. https://doi.org/10.1007/s00401-015-1404-5.

Bartlomiejczyk, M.A., Swierzko, A.S., Brzostek, A., Dziadek, J., Cedzynski, M., 2014. Interaction of lectin pathway of complement-activating pattern recognition molecules with Mycobacteria. Clin. Exp. Immunol. 178, 310–319. https://doi.org/10.1111/cei.12416.

Benjamini, Y., Krieger, A.M., Yekutieli, D., 2006. Adaptive linear step-up procedures that control the false discovery rate. Biometrika 93, 491–507. https://www.jstor.org/stable/20441303.

Besra, G.S., 1998. Preparation of cell-wall fractions from mycobacteria. Methods in molecular biology (Clifton, NJ) 101, 91–107. https://doi.org/10.1385/0-89603-471-2:91.

Birch, H.L., Alderwick, L.J., Appelmelk, B.J., Maaskant, J., Bhatt, A., Singh, A., Nigou, J., Eggeling, L., Geurtsen, J., Besra, G.S., 2010. A truncated lipoglycan from mycobacteria with altered immunological properties. In: Proceedings of the National Academy of Sciences of the United States of America 107:2634–9. https://doi.org/10.1073/pnas.0915082107.

Borders, C.W., Courtney, A., Ronen, K., Laborde-Lahoz, M.P., Guidry, T.v., Hwang, S.A., Olsen, M., Hunter, R.L., Hollmann, T.J., Wetsel, R.A., Actor, J.K., 2005. Requisite role for complement C5 and the C5a receptor in granulomatous response to mycobacterial glycolipid trehalose 6,6′-dimycolate. Scand. J. Immunol. 62, 123–130. https://doi.org/10.1099/mic.0.2008/016923-0.

Briken, V., Porcelli, S.A., Besra, G.S., Kremer, L., 2004. Mycobacterial lipoarabinomannan and related lipoglycans: From biogenesis to modulation of the immune response. Mol. Microbiol. 53 (2), 391–403. https://doi.org/10.1111/j.1365-2958.2004.04183.x.

Brookes, C., Freire-Martin, I., Cavell, B., Alexander, F., Taylor, S., Persaud, R., Fry, N., Preston, A., Diavatopoulos, D., Gorringe, A., 2018. Bordetella pertussis isolates vary in their interactions with human complement components article. Emerging Microbes Infect. 7 (1), 81. https://doi.org/10.1038/s41426-018-0084-3.

Cai, Y., Yang, Q., Tang, Y., Zhang, M., Liu, H., Zhang, G., Deng, Q., Huang, J., Gao, Z., Zhou, B., Feng, C.G., Chen, X., 2014. Increased Complement C1q Level Marks Active Disease in Human Tuberculosis. PLoS ONE 9, e92340. https://doi.org/10.1371/journal.pone.0092340.

Cywes, L., Hoppe, H.C., Daffé, M., Ehlers, M.R.W., 1997. Nonopsonic binding of *Mycobacterium tuberculosis* to complement receptor type 3 is mediated by capsular polysaccharides and is strain dependent. Infect. Immun. 65, 4258–4266.

Domenech, M., Ramos-Sevillano, E., García, E., Moscoso, M., Yuste, J., 2013. Biofilm formation avoids complement immunity and phagocytosis of *Streptococcus pneumoniae*. Infect. Immun. 81, 2606–2615. https://doi.org/10.1128/IAI.00491-13.

Fletcher, H.A., Schrager, L., 2016. TB vaccine development and the End TB Strategy: Importance and current status. Trans. R. Soc. Trop. Med. Hyg. 110, 212–218. https://doi.org/10.1093/trstmh/trw016.

Ferguson, J.S., Weis, J.J., Martin, J.L., Schlesinger, L.S., 2004. Complement protein C3 binding to Mycobacterium tuberculosis is initiated by the classical pathway in human bronchoalveolar lavage fluid. Infect. Immun. 72, 2564–2573. https://doi.org/10.1093/trstmh/trw016.

Gago, G., Diacovich, L., Gramajo, H., 2018. Lipid metabolism and its implication in mycobacteria–host interaction. Curr. Opin. Microbiol. 41, 36–42. https://doi.org/10.1016/j.mib.2017.11.020.

Gout, E., Garlatti, V., Smith, D.F., Lacroix, M., Dumestre-Pérard, C., Lunardi, T., Martin, L., Cesbron, J.Y., Arlaud, G.J., Gaboriaud, C., Thielens, N.M., 2010. Carbohydrate recognition properties of human ficolins: Glycan array screening reveals the sialic acid binding specificity of M-ficolin. J. Biol. Chem. 285, 6612–6622. https://doi.org/10.1074/jbc.M109.065854.

Grosset, J., 2003. *Mycobacterium tuberculosis* in the extracellular compartment: An underestimated adversary. Antimicrobial Agents and Chemotherapy. Antimicrob Agents Chemother. 47 (3), 833–836. https://doi.org/10.1128/AAC.47.3.833-836.2003.

Hoff, D.R., Ryan, G.J., Driver, E.R., Ssemakulu, C.C., de Groote, M.A., Basaraba, R.J., Lenaerts, A.J., 2011. Location of intra- and extracellular M. tuberculosis populations in lungs of mice and guinea pigs during disease progression and after drug treatment. PLoS ONE 6 (3). https://doi.org/10.1371/journal.pone.0017550.

Hunter, R.L., 2016. Tuberculosis as a three-act play: A new paradigm for the pathogenesis of pulmonary tuberculosis. Tuberculosis 97, 8–17. https://doi.org/10.1016/j.tube.2015.11.010.

Hunter, R.L., 2011. Pathology of post primary tuberculosis of the lung: An illustrated critical review. Tuberculosis. Tuberculosis (Edinb). https://doi.org/10.1016/j.tube.2011.03.007.

Jagannath, C., Hoffmann, H., Sepulveda, E., Actor, J.K., Wetsel, R.A., Hunter, R.L., 2000. Hypersusceptibility of A/J mice to tuberculosis is in part due to a deficiency of the fifth complement component (C5). Scand. J. Immunol. 52, 369–379. https://doi.org/10.1046/j.1365-3083.2000.00770.x.

James, B.W., Williams, A., Marsh, P.D., 2000. The physiology and pathogenicity of Mycobacterium tuberculosis grown under controlled conditions in a defined medium. J. Appl. Microbiol. 88, 669–677. https://doi.org/10.1046/j.1365-2672.2000.01020.x.

Jensen, E.T., Kharazmi, A., Garred, P., Kronborg, G., Fomsgaard, A., Mollnes, T.E., Høiby, N., 1993. Complement activation by pseudomonas aeruginosa biofilms. Microb. Pathog. 15, 377–388. https://doi.org/10.1006/mpat.1993.1087.

Kharazmi, A., 1991. Mechanisms involved in the evasion of the host defence by Pseudomonas aeruginosa. Immunol. Lett. 30, 201–205. https://doi.org/10.1016/0165-2478(91)90026-7.

Lanoix, J.P., Lenaerts, A.J., Nuermberger, E.L., 2015. Heterogeneous disease progression and treatment response in a C3HeB/FeJ mouse model of tuberculosis. DMM Disease Models and Mechanisms 8, 603–610. https://doi.org/10.1242/dmm.019513.

Lemassu, A., Daffe, M., 1994. Structural features of the exocellular polysaccharides of Mycobacterium tuberculosis. Biochem. J. 297, 351–357. https://doi.org/10.1042/bj2970351.

Lenaerts, A., Barry, C.E., Dartois, V., 2015. Heterogeneity in tuberculosis pathology, microenvironments and therapeutic responses. Immunol. Rev. 264, 288–307. https://doi.org/10.1111/imr.12252.

Lenaerts, A.J., Hoff, D., Aly, S., Ehlers, S., Andries, K., Cantarero, L., Orme, I.M., Basaraba, R.J., 2007. Location of persisting mycobacteria in a guinea pig model of tuberculosis revealed by R207910. Antimicrob. Agents Chemother. 51, 3338–3345. https://doi.org/10.1128/AAC.00276-07.

Limoli DH, Jones CJ, Wozniak DJ. 2015. Bacterial Extracellular Polysaccharides in Biofilm Formation and Function. Microbiology Spectrum, 01 Jun 2015, 3(3). 10.1128/microbiolspec.mb-0011-2014.

Malik, Z.A., Denning, G.M., Kusner, D.J., 2000. Inhibition of Ca2+ signaling by Mycobacterium tuberculosis is associated with reduced phagosome-lysosome fusion and increased survival within human macrophages. J. Exp. Med. 191, 287–302. https://doi.org/10.1128/AAC.00276-07.

Mashruwala, M.A., Smith, A.K., Lindsey, D.R., Moczygemba, M., Wetsel, R.A., Klein, J.R., Actor, J.K., Jagannath, C., 2011. A defect in the synthesis of Interferon-γ by the T cells of Complement-C5 deficient mice leads to enhanced susceptibility to tuberculosis. Tuberculosis 91, S82. https://doi.org/10.1016/j.tube.2011.10.016.

N'Diaye, E.N., Darzacq, X., Astarie-Dequeker, C., Daffé, M., Calafat, J., Maridonneau-Parini, I., 1998. Fusion of azurophil granules with phagosomes and activation of the tyrosine kinase Hck are specifically inhibited during phagocytosis of mycobacteria by human neutrophils. J. Immunol. (Baltimore, Md : 1950) 161:4983–91.

Nyka, W., 1967. Method for staining both acid-fast and chromophobic tubercle bacilli with carbolfuschsin. J. Bacteriol. 93, 1458–1460. https://doi.org/10.1128/jb.93.4.1458-1460.1967.

Nyka, W., 1974. Studies on the effect of starvation on mycobacteria. Infect. Immun. 9, 843–850. https://doi.org/10.1128/iai.9.5.843-850.1974.

Nyka, W., O'Neill, E.F., 1970. A new approach to the study of non-acid-fast mycobacteria. Ann. N. Y. Acad. Sci. 174, 862–871. https://doi.org/10.1111/j.1749-6632.1970.tb45605.x.

Ojha, A.K., Baughn, A.D., Sambandan, D., Hsu, T., Trivelli, X., Guerardel, Y., Alahari, A., Kremer, L., Jacobs, W.R., Hatfull, G.F., 2008. Growth of Mycobacterium tuberculosis biofilms containing free mycolic acids and harbouring drug-tolerant bacteria. Mol. Microbiol. 69, 164–174. https://doi.org/10.1111/j.1365-2958.2008.06274.x.

Ortalo-Magné, A., Dupont, M.A., Lemassu, A., Andersen, A.B., Gounon, P., Daffé, M., 1995. Molecular composition of the outermost capsular material of the tubercle bacillus. Microbiology 141 (7), 1609–1620. https://doi.org/10.1099/13500872-141-7-1609.

Queiroz, A., Riley, L.W., 2017. Bacterial immunostat: Mycobacterium tuberculosis lipids and their role in the host immune response. Rev. Soc. Bras. Med. Trop. 50 (1), 9–18. https://doi.org/10.1590/0037-8682-0230-2016.

Rhoades, E.R., Archambault, A.S., Greendyke, R., Hsu, F.-F., Streeter, C., Byrd, T.F., 2009. Mycobacterium abscessus glycopeptidolipids mask underlying cell wall phosphatidyl-myo-inositol mannosides blocking induction of human macrophage TNF-α by preventing interaction with TLR2. J. Immunol. 183, 1997–2007. https://doi.org/10.4049/jimmunol.0802181.

Romero, M.M., Duarte, A., Pastorini, M., Alemán, M., 2019. Role of α-glucan-induced oxygen species in dendritic cells and its impact in immune response against tuberculosis. Int. J. Med. Microbiol. 309 (6), 151328 https://doi.org/10.1016/j.ijmm.2019.07.002.

Schlesinger, L.S., Bellinger-Kawahara, C.G., Payne, N.R., Horwitz, M.A., 1990. Phagocytosis of Mycobacterium tuberculosis is mediated by human monocyte complement receptors and complement component C3. J. Immunol. (Baltimore, Md : 1950) 144:2771–80.

Schwebach, J.R., Glatman-Freedman, A., Gunther-Cummins, L., Dai, Z., Robbins, J.B., Schneerson, R., Casadevall, A., 2002. Glucan is a component of the Mycobacterium tuberculosis surface that is expressed in vitro and in vivo. Infect. Immun. 70, 2566–2575. https://doi.org/10.1128/IAI.70.5.2566-2575.2002.

Strunk, R.C., Eidlen, D.M., Mason, R.J., 1988. Pulmonary alveolar type II epithelial cells synthesize and secrete proteins of the classical and alternative complement pathways. J. Clin. Invest. 81, 1419–1426. https://doi.org/10.1172/JCI113472.

Świerzko, A.S., Bartłomiejczyk, M.A., Brzostek, A., Łukasiewicz, J., Michalski, M., Dziadek, J., Cedzyński, M., 2016. Mycobacterial antigen 85 complex (Ag85) as a target for ficolins and mannose-binding lectin. Int. J. Med. Microbiol. 306, 212–221. https://doi.org/10.1016/j.ijmm.2016.04.004.

Villeneuve, C., Etienne, G., Abadie, V., Montrozier, H., Bordier, C., Laval, F., Daffe, M., Maridonneau-Parini, I., Astarie-Dequeker, C., 2003. Surface-exposed glycopeptidolipids of Mycobacterium smegmatis specifically inhibit the phagocytosis of mycobacteria by human macrophages. Identification of a novel family of glycopeptidolipids. J. Biol. Chem. 278, 51291–51300. https://doi.org/10.1074/jbc.M306554200.

Volanakis, J.E., Barnum, S.R., Giddens, M., Galla, J.H., 1985. Renal filtration and catabolism of complement protein D. N. Engl. J. Med. 312, 395–399. https://doi.org/10.1056/NEJM198502143120702.

Vogt, S., Trendelenburg, M., Tamm, M., Stolz, D., Hostettler, K.E., Osthoff, Michael, 2020. Local and systematic concentrations of pattern recognition receptors of the lectin pathway of complement in a cohort of patients with interstitial lung disease. Front. Immunol 23 (11), 562564. https://doi.org/10.3389/fimmu.2020.562564.

Watford, W.T., Ghio, A.J., Wright, J.R., 2000. Complement-mediated host defense in the lung. Am. J. Physiol. Lung Cell Mol. Physiol. 279, L790–L798. https://doi.org/10.1152/ajplung.2000.279.5.L790.

Welsh, K.J., Lewis, C.T., Boyd, S., Braun, M.C., Actor, J.K., 2012. Complement factor C7 contributes to lung immunopathology caused by mycobacterium tuberculosis. Clinical and Developmental Immunology 2012. https://doi.org/10.1155/2012/429675.

Welsh, K.J., Abbott, A.N., Hwang, S.A., Indrigo, J., Armitige, L.Y., Blackburn, M.R., Hunter, R.L., Actor, J.K., 2008. A role for tumour necrosis factor-α, complement C5 and interleukin-6 in the initiation and development of the mycobacterial cord factor trehalose 6,6′-dimycolate induced granulomatous response. Microbiology 154, 1813–1824. https://doi.org/10.1099/mic.0.2008/016923-0.